Journal of Macromolecular Science, Part B: Physics

Publication details, including instructions for authors and subscription information:
http://www.tandfonline.com/loi/lmsb20

Comparison of Lattice-Fluid Binary Parameters For Mixtures and Block Copolymers

Carmen C. Riccardi [a], Walter F. Schroeder [a], Elena Serrano [b] & Iñaki Mondragon [c]

[a] Institute of Materials Science and Technology (INTEMA), University of Mar de Plata and National Research Council (CONICET), Mar de Plata, Argentina

[b] Molecular Nanotechnology Laboratory, University of Alicante, Campus de San Vicente, Alicante, Spain

[c] Group "Materials + Technologies," Polytechnic School, Departmento Ingenieria Quimica y M. Ambiente, Universidad Pais Vasco/Euskal Herriko Unibertsitatea, Donostia-San Sebastian, Spain

Accepted author version posted online: 18 Apr 2012.Version of record first published: 16 Oct 2012.

To cite this article: Carmen C. Riccardi, Walter F. Schroeder, Elena Serrano & Iñaki Mondragon (2013): Comparison of Lattice-Fluid Binary Parameters For Mixtures and Block Copolymers, Journal of Macromolecular Science, Part B: Physics, 52:1, 65-83

To link to this article: http://dx.doi.org/10.1080/00222348.2012.685829

Journal of Macromolecular Science®, Part B: Physics, 52:65–83, 2013

ISSN: 0022-2348 print / 1525-609X online
DOI: 10.1080/00222348.2012.685829

Comparison of Lattice-Fluid Binary Parameters For Mixtures and Block Copolymers

CARMEN C. RICCARDI,[1] WALTER F. SCHROEDER,[1] ELENA SERRANO,[2] AND IÑAKI MONDRAGON[3]

[1]Institute of Materials Science and Technology (INTEMA), University of Mar de Plata and National Research Council (CONICET), Mar de Plata, Argentina
[2]Molecular Nanotechnology Laboratory, University of Alicante, Campus de San Vicente, Alicante, Spain
[3]Group "Materials + Technologies," Polytechnic School, Departmento Ingenieria Quimica y M. Ambiente, Universidad Pais Vasco/Euskal Herriko Unibertsitatea, Donostia–San Sebastian, Spain

The aim of this report is to discuss the method of determination of lattice-fluid binary interaction parameters by comparing well characterized immiscible blends and block copolymers of poly(methyl methacrylate) (PMMA) and poly(ε−caprolactone) (PCL). Experimental pressure-volume-temperature (PVT) data in the liquid state were correlated with the Sanchez—Lacombe (SL) equation of state with the scaling parameters for mixtures and copolymers obtained through combination rules of the characteristic parameters for the pure homopolymers. The lattice-fluid binary parameters for energy and volume were higher than those of block copolymers implying that the copolymers were more compatible due to the chemical links between the blocks. Therefore, a common parameter cannot account for both homopolymer blend and block copolymer phase behaviors based on current theory. As we were able to adjust all data of the mixtures with a single set of lattice-binary parameters and all data of the block copolymers with another single set we can conclude that both parameters did not depend on the composition for this system. This characteristic, plus the fact that the additivity law of specific volumes can be suitably applied for this system, allowed us to model the behavior of the immiscible blend with the SL equation of state. In addition, a discussion on the relationship between lattice-fluid binary parameters and the Flory–Huggins interaction parameter obtained from Leibler's theory is presented.

Keywords block copolymer, immiscible blend, interaction parameter, lattice-binary parameter, PVT

1. Introduction

Most of the studies of polymer–polymer phase behavior assume that homopolymer mixtures and block copolymer melts are controlled by a common segment–segment interaction parameter known as the Flory–Huggins' phenomenological interaction parameter, χ.[1,2]

Received 30 November 2011; accepted 4 April 2012.
Address correspondence to Carmen C. Riccardi, Institute of Materials Science and Technology (INTEMA), University of Mar de Plata and National Research Council (CONICET), Av. Juan B. Justo 4320, B7608FQD Mar de Plata, Argentina. E-mail: criccard@fi.mdp.edu.ar

There are relatively few examples of experimental studies that have simultaneously quantified block copolymer and homopolymer mixture phase behaviors. Lohse and coworkers[3] studied blends of polyethylene and polypropylene in comparison with poly(ethylene-*b*-propylene) block copolymers and concluded that a single χ-parameter could be used to describe the phase behavior of these systems. However, Maurer et al.[4] pointed out that the experimental error in this type of isothermal study could accommodate up to a twofold difference between blend and diblock copolymer interaction parameters. Even more, from the comparison of the Flory–Huggins interaction parameter obtained for a polyethylene–polypropylene blend with the χ-parameter obtained for the homologous block copolymer, extracted from order–disorder transition temperature (TODT) data, they concluded that the current theories cannot account for both homopolymer blend and block copolymer phase behaviors.[5]

The lattice theory of Sanchez—Lacombe (SL)[6,7] has been applied extensively to both homopolymers blends[8–12] and copolymers[13–15] using pressure-volume-temperature (PVT) data to determine the interaction parameter. In the framework of this theory, scaling parameters of pure components are obtained by fitting PVT data, while model parameters of miscible mixtures or block copolymers are calculated by using mixing rules as a function of lattice-binary interaction parameters. There is some controversy in the literature concerning the relationship between the χ-parameter and the lattice-fluid binary parameters. While some authors relate the SL lattice-fluid binary parameters with the Flory–Huggins χ-parameter,[16–18] other authors relate the former parameters with the integral Flory–Huggins interaction parameter or residual energy of mixing, g.[11,19] In both cases, the relationship between the parameters is obtained by equating the mixing Gibbs free energy expressed through the respective theories. Callaghant and Paul[9] calculated interaction energies for each one of the binary pairs of poly(styrene) (PS), poly(methyl styrene) (PMS), and poly(methyl methacrylate) (PMMA) by fitting spinodal curves predicted by the Flory–Huggins theory and the SL equation of state to experimental cloud point data of low molecular weight polymer blends. They concluded that, while interaction energies calculated from the theories of SL and Flory–Huggins are essentially equal for the PS/PMS pair when the upper and lower estimates are averaged, the corresponding values for PMMA with PS or PMS are different due to the difference in their characteristic temperatures.

Most of the published works propose the modeling of PVT data of the miscible zone to predict spinodal and binodal curves of blends.[11,20–22] Sato et al. studied the miscibility and volume changes of mixing in poly(vinyl chloride)/PMMA blends,[23] and specific volumes as a function of the number of carbon atoms in branched chains of polyethylene copolymer melts.[15] When an equation of state was used to predict the mixing behavior of two substances that give place to a homogeneous solution, one assumes that both mixture and components obey the same equation of state, that the hard-core volumes are additive and that there are parameters that can take into account interactions between the molecules.[24] To our knowledge, the modeling of PVT data of immiscible mixtures has not been done. In addition to the requirements for miscible blends, the Flory–Huggins or lattice-fluid parameters should be the same for both phases in immiscible blends, which means that they must not depend on the composition.

With the aim to compare binary lattice-fluid parameters of immiscible blends and block copolymers of the same components, we have studied mixtures and corresponding diblock copolymers of PMMA and poly(ε-caprolactone) (PCL). The interest in blends of PCL with other polymers stems from its biodegradability and their potential use in biomedical applications. Because of its low glass transition temperature along with its biodegradability,

blends of PCL with other polymers have been of interest. In contrast to PCL, which is semicrystalline, PMMA is an amorphous polymer that has also a wide range of utilization areas, including biomedical implants such as replacement for intraocular lenses, bone cements, and dentures. The combination of biostable PMMA and biodegradable PCL polymers provides interesting materials with good mechanical integrity.[25–27]

2. Experimental

2.1. Materials

ε-Caprolactone (CL) can be polymerized by ring-opening polymerization (ROP) whereas methyl methacrylate (MMA) can be polymerized by atom-transfer radical polymerization.[28] Eight semicrystalline poly(methyl methacrylate-*b*-ε-caprolactone) (PMMA-*b*-PCL) diblock copolymers (MC) were synthesized following a two step route previously reported in the literature.[29,30] ε-Caprolactone was homopolymerized by a ROP technique. Two different PCL homopolymers with different molecular weight (PCL14 and PCL27, see Table 1) were prepared and functionalized with methyl-α-bromo isobutyrate to be used as precursors for the polymerization of MMA. In the second step, MMA monomer was polymerized by atom-transfer radical polymerization on the functionalized PCL.[31] The PCL macroinitiator, dibromo bis(triphenylphosphine) nickel(II) catalyst, and dry MMA were charged into a previously evacuated flask and allowed to stir at room temperature until the macroinitiator dissolved. Tetrahydrofuran (THF) was added to the mixture to facilitate the dissolution of the initiator and to reduce the viscosity during polymerization. The reaction flask was then placed in an oil bath at 80°C and allowed to react for about 5 h. The block copolymer was extracted with hexane, then precipitated in methanol, isolated by filtration, and finally dried under reduced pressure.

The MC1 to MC4 block copolymers were prepared from the same poly(ε-caprolactone) precursor (PCL14), while MC5 to MC8 samples were prepared from the PCL 27 precursor. A PMMA homopolymer (PMMA13) and three PMMA13-PCL14 mixtures (M1, M2, and M3 with PMMA mass fraction equal to 0.25, 0.55, and 0.75, respectively), were also

Table 1
Molecular characterization of the polymers by GPC

Sample	M_n 10^4 (g mol^{-1})	M_w 10^4 (g mol^{-1})	PDI
PMMA13	1.32	2.24	1.70
PCL14	1.42	2.15	1.52
PCL27	2.67	3.25	1.21
MC1	2.72	3.88	1.42
MC2	3.87	6.06	1.56
MC3	5.29	9.66	1.83
MC4	7.02	9.48	1.35
MC5	3.39	4.13	1.22
MC6	3.99	4.96	1.24
MC7	4.75	6.01	1.27
MC8	5.37	7.18	1.34

Table 2
Molecular parameters of the synthesized diblock copolymers and mixtures

Copolymer	N_{PMMA}/N_{PCL}	N_{PMMA}	N	ϕ_{PMMA}	w_{PMMA}
MC1	1.43	156.5	281.8	0.53	0.55
MC2	2.66	250.7	275.2	0.68	0.70
MC3	3.48	380.3	504.8	0.73	0.75
MC4	5.60	611.9	736.5	0.84	0.83
MC5	0.47	98.3	335.2	0.28	0.29
MC6	0.95	196.7	433.5	0.44	0.45
MC7	1.55	322.7	559.6	0.56	0.58
MC8	1.75	362.9	599.7	0.58	0.61
M1	–	–	–	0.24	0.25
M2	–	–	–	0.53	0.55
M3	–	–	–	0.73	0.75

studied. The mixtures were prepared using dichloromethane to facilitate the mixing process, followed by solvent evaporation at 40°C under reduced pressure until the theoretical constant weight was achieved. The molecular parameter values for all the components used in this study are reported in Tables 1 and 2.

2.2. Characterization Techniques

Polymer molecular weights and molecular weight distributions were measured by gel permeation chromatography (GPC) using a liquid chromatograph (S-250, Perkin–Elmer, USA) equipped with a UV detector (LC-235 UV, Perkin–Elmer, USA) and a refractive index detector (LC-30 RI, Perkin-Elmer, USA). Three Waters Styragel columns (HR 2, HR 4, and HR 5E; USA) were used with THF as the elution solvent at a flow rate of 1 mL min^{-1} at 25°C. Calibration was performed using polystyrene standards due to absence of Mark–Houwink constants for these block copolymers in THF.

Copolymer compositions were determined by ^{1}H-nuclear magnetic resonance (^{1}H NMR) spectroscopy. The ^{1}H NMR spectra were recorded with a Bruker 500 MHz spectrometer (Bruker Corporation, USA) using deuterated chloroform as solvent and tetramethylsilane as an internal reference.

A *PVT* analyzer (SWO/Haake PVT 100, Thermo Fisher, USA) was used to measure specific volume of the samples, v, as a function of temperature and pressure. The instrument covers a temperature and pressure range from 25 to 400°C and 200–2500 bar, respectively, with 1 bar data being extrapolated from pressure data. Isobaric experiments were carried out from 200 to 600 bars with 200 bar steps. Specific volume measurements were recorded from 150°C until 30°C, with a cooling rate of 5°C min^{-1}.

Dynamic oscillatory shear measurements were performed using a rheometer (Rheometrics Ares, TA Instruments, USA) equipped with 25 mm diameter parallel plates and a transducer with an operating range of 0.02–200 g cm with the aim to determine the apparent order–disorder transition temperatures, ($TODT_{app}$). The parallel plates were calibrated to correct for thermal expansion. Samples of 13 mm diameter and around 1 mm of thickness were made by pressing the sample at 165°C in a press with a force of 10 ton. After loading the sample in the rheometer, it was heated to 195°C for 10 min to erase all prior

themomechanical history. The sample was then cooled ensuring always that the normal force was close to zero, so as not to induce any macroscopic alignment of the sample. Dynamic isochronal temperature scans were performed at a frequency of 6.28 rad s^{-1}. The temperature range used for dynamic scans was from 40 to 240°C, ensuring that the sample did not degrade thermally.

Transmission optical microscopy (TOM) was used to follow the evolution of phases after the melting process of PCL. A microscope (Leica DMLB, Germany) provided with a video camera (Leica DC 100, Germany) and a hot stage (THMD 600, Linkman Scientific Instruments Ltd., England) was employed. Optical transmittance measurements in the wavelength of visible light were made using a photodetector incorporated into the optical path of the microscope.

3. Results and Discussion

3.1. Characterization

3.1.1. Molecular characterization. Gel permeation chromatography was used to determine the molecular characteristics of the samples. Number and weight average molecular weights, M_n and M_w, and the polydispersity index, PDI $= M_w/M_n$, are shown in Table 1.

The ^{1}H Nuclear magnetic resonance was used to determine the composition of each copolymer. Figure 1 shows the spectra of the MC7 block copolymer, as a sample, and the peak assignments in accord with published results.[32–35] From the ^{1}H NMR spectra, the ratio between the numbers of monomers of each polymer, N_{PMMA}/N_{PCL}, was obtained using

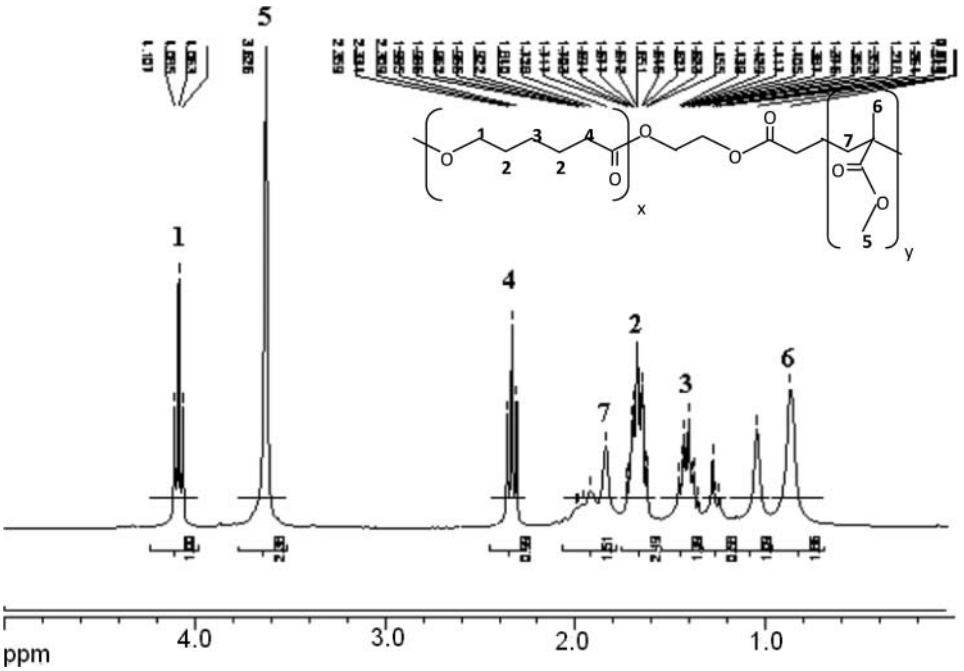

Figure 1. ^{1}H NMR spectra of MC7 copolymer and its corresponding peak assignments.

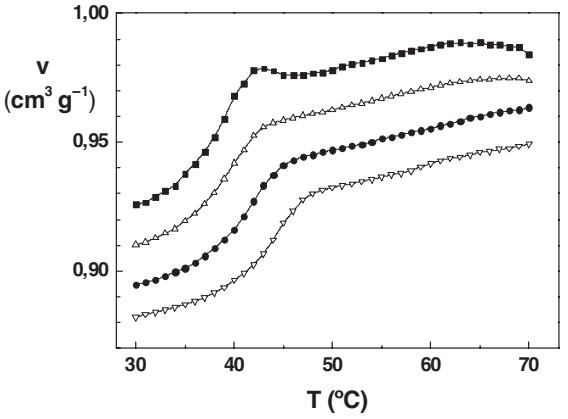

Figure 2. PVT scan of PCL14 at different pressures: (■) 0.1, (△) 20, (●) 40 and (▽) 60 MPa.

the peak areas $A_{3,6}$ and $A_{4,1}$ corresponding to the signals of $–CH_3$ of PMMA and $–OCH_2–$ of PCL, respectively.

Combining ^{1}H RMN and GPC data, the number of repeat units in the PMMA block, N_{PMMA}, in the PCL block, M_{PCL}, and in the copolymer, N, were obtained. Furthermore, the volume fractions of the PMMA block, ϕ_{PMMA}, were calculated using the densities of the homopolymers at 25°C ($\rho_{PMMA} = 1.09$ g cm^{-3}, ρ_{PCL} [fully amorphous] $= 1.188$ g cm^{-3})[36] and the expression derived by Helfand.[37] Results for each copolymer are summarized in Table 2.

3.1.2. The PVT characterization. The PVT scans for the PCL14 and PMMA13 homopolymers are shown in Figs. 2 and 3 respectively. The melting process of PCL can be seen in Fig. 2. By the intercepts of the tangents of the curves at the beginning and the end of the melting process the onset and the end melting temperature, T_{mO} and T_{mE} respectively, were determined and listed in Table 3. It is worth noting that T_{mO} and T_{mE} increased for higher pressures. In addition, the changes of melting temperatures with pressure were very similar for the onset and the end ones: 0.101 and 0.092 K MPa^{-1}, respectively. The pressure

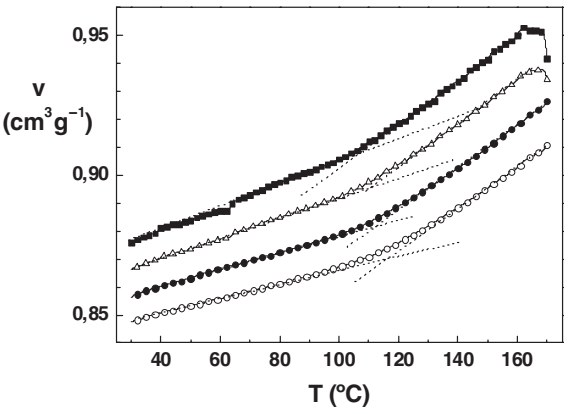

Figure 3. PVT scans of PMMA13 at different pressures: (■) 0.1, (△) 20, (●) 40 and (▽) 60 MPa.

Table 3
The PVT parameters of homopolymers as a function of pressure

	PCL14		PMMA13
P (Mpa)	T_{mO} (°C)	T_{mE} (°C)	T_g (°C)
0.1	34.5	41.7	102.3
20	35.8	43.1	104.5
49	38.3	44.9	111.9
60	40.4	47.2	114.7

dependence of the melting point of a number of polymers, including homo- and copolymers (HDPE, LDPE, PP, and ethylene vinyl acetate copolymers [EVA]), has been found to be in the range of 0.11 to 0.17 K MPa^{-1}.[38] Our values are lower but of the same order.

The glass transition temperatures of PMMA, T_g, were determined from intercepts of the tangents of the curves shown in Fig. 3. The obtained results are listed in Table 3. Their values present a linear trend with pressure (not shown), as it has also been reported for polystyrene and its copolymers with maleic anhydride.[39] The slope of the linear relation between T_g and pressure was 0.254 K MPa^{-1}, close to that reported by Wang et al. (0.238 K MPa^{-1}).[40] In addition, the T_g value at atmospheric pressure (102.3°C) agrees with the value reported by Kilburn et al. (103°C) from PVT experiments.[41]

Figure 4 shows PVT scans at 0.1 MPa for the mixtures M1, M2, and M3. As PCL content was decreased in the mixture, the melting process became less significant. The comparison of the PVT behavior of a block copolymer and a mixture with the same PMMA mass fraction is shown in Fig. 5 for copolymer MC1 and mixture M2, both with 55 wt% PMMA, at 0.1 MPa. Whereas the PVT scan of the block copolymer shows the characteristic features of the behavior of each block, the scan of the mixture shows the shift of the melting process and the T_g toward higher and lower temperatures respectively. Similar results occurred for the other compositions.

The T_g values of PMMA in mixtures and block copolymers, as a function of pressure, are listed in Table 4. The T_g values of the PMMA blocks were more or less the same for each

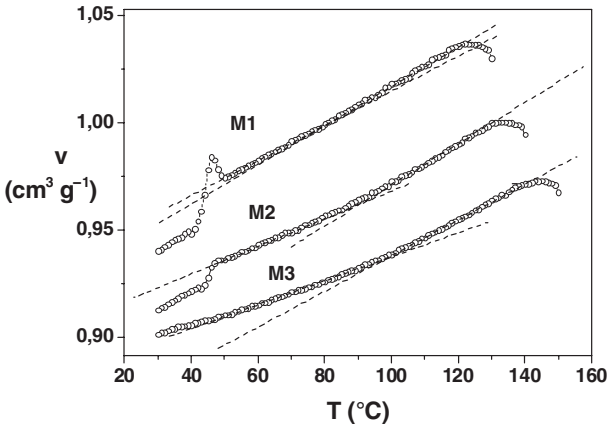

Figure 4. Comparative PVT scans at 0.1 MPa for mixtures M1 to M3.

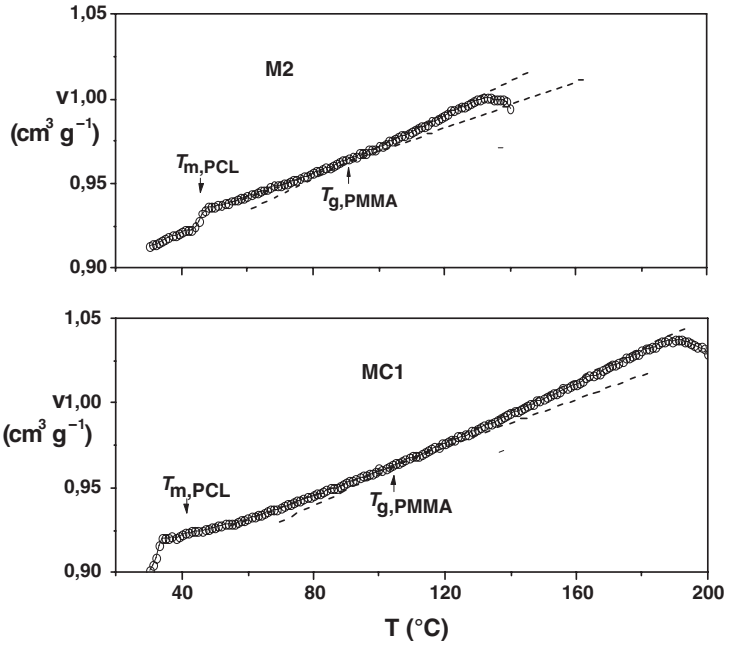

Figure 5. PVT scans at 0.1 MPa of a mixture and a block copolymer with same composition, $w_{PMMA} = 0.55$.

copolymer and agree with previously reported results.[41] The value at 0.1 MPa, averaged from all samples, was equal to 104.4°C, coincidental with the value obtained by DSC.[42] Figure 6 shows the averaged T_g values vs. pressure; they have a slope of 0.221 K MPa^{-1}, close to that of PMMA homopolymer (0.194 K MPa^{-1}).

The T_g values for the mixtures were lower than those of the corresponding block copolymers, as seen in Table 4. This effect is a consequence of the PCL content dissolved in the PMMA-rich phase (α). The mass fractions of PCL in the PMMA-rich domains in the mixtures (w^{α}_{PCL}) were obtained by applying the Fox equation[43] for the glass transition temperature determined at 0.1 MPa and taking into account that the T_g of PCL is −63°C.[44] The calculated values of w^{α}_{PCL} were: 0.076 for M1, 0.038 for M2, and 0.014 for M3. Note that the mass fraction of PCL in the PMMA-rich phase increased with the

Table 4
The T_g values of PMMA in mixtures and block copolymers as a function of pressure

	$T_{g\ PMMA}$ (°C)								
	Mixtures			*Block copolymers*					
P (MPa)	M1	M2	M3	MC1	MC2	MC3	MC4	MC7	MC8
0.1	81.2	92.2	98.3	103.6	105.0	105.6	100.4	105.9	105.9
20	82.8	98.5	100.6	107.1	109.6	110.3	106.6	107.9	109.2
40	85.8	105.3	113.9	110.9	113.9	114.5	113.0	114.0	112.9
60	88.6	108.4	116.2	116.4	116.2	117.0	119.0	118.4	117.0

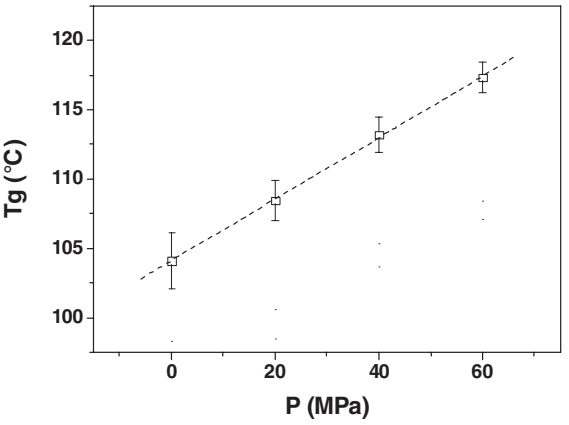

Figure 6. Glass transition temperature of PMMA block as a function of pressure from PVT data.

global concentration of PCL in the mixture. Similar results were obtained by extrapolation from DSC thermograms published for mixtures of PCL and PMMA by Iannace et al.[27]

3.1.3. Rheological characterization of the copolymers. Dynamic isochronal temperature scans of the storage modulus, G′, at a frequency of 6.28 rad s^{-1} for the block copolymers are shown in Fig. 7. These scans were taken above the melting temperature, T_m, of the PCL block, and thus the magnitudes of both G′ and G″ were expected to be nearly constant up to the glass transition temperature of the PMMA block. Except for the lower molecular weight block copolymer, MC5, a gradual drop in the magnitude of G′ that finally approached to a plateau value can be observed around 110°C, which corresponds to the α relaxation mode for the PMMA block which can be associated with its T_g. At higher temperatures a second drop in the magnitude of G′ occurred. It can be clearly observed that the T_g of the PMMA block, the plateau region and the fall of G' magnitude diminished as molecular weight of MC copolymers decreased. In the case of the MC5 block copolymer, both the T_g and the second drop of G′ apparently overlapped probably due to its low molecular mass. Following

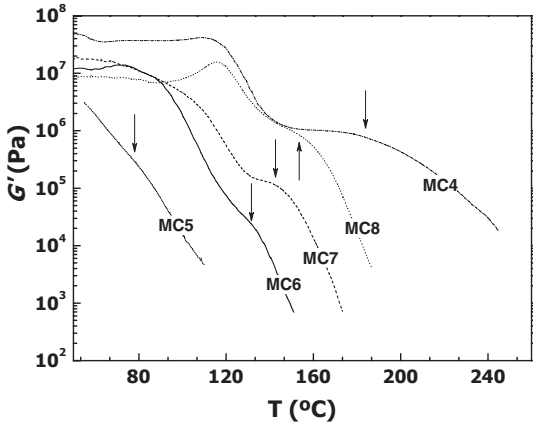

Figure 7. Dynamic isochronal temperature dependence of the storage modulus at a frequency of 6.28 rad s^{-1} for several block copolymers. Arrows indicate TODTapp.

Table 5
Order-disorder transition temperatures of the block copolymers

Block copolymer	ϕ_{PMMA}	$TODT_{app}$ (°C)	$\chi N_{LEIBLER}$	N
MC4	0.83	187.7 ± 5.7	31.45	736.5
MC5	0.29	81.4 ± 3.7	15.14	335.2
MC6	0.40	123.4 ± 8.4	10.70	433.5
MC7	0.58	147.2 ± 4.8	11.30	559.6
MC8	0.61	162.1 ± 4.5	11.54	599.7

the rheological criteria [45,46] that the temperature at which G′ begins to abruptly drop in the plot of log G′ vs. temperature signifies the order–disorder transition, we can determine the $TODT_{app}$ for MC block copolymers, which are indicated by arrows in Fig. 7. These temperatures have allowed us to compare the binary lattice fluid parameters with the Flory's interaction parameter.

The $TODT_{app}$ for the MC block copolymers are shown in Table 5. The TODT decreased as volumetric fraction of PMMA did. Similar results were obtained by studying the order–disorder transition of a series of symmetric poly(oxyethylene-*b*-oxypropylene)[45] and a series of eleven diblock copolymers of poly(oxyethylene-*b*-oxybutylene).[46]

3.1.4. Optical characterization of the mixtures. The mixtures were phase separated in the range of 50–200°C, as observed in the optical microscopy photograph of M1 shown in Fig. 8. This mixture had a phase (α) rich in PMMA with a volume fraction, ϕ^{α}, of 0.224 calculated by image analysis. As previously mentioned, the mass fraction of PCL in the PMMA-rich domains ($w^{\alpha}{}_{PCL}$) in the mixture M1 was equal to 0.076. Consequently, the mass fraction of PMMA in the α phase ($w^{\alpha}{}_{PMMA}$) was 0.924.

The composition of the β phase and the total mass fraction of the α-phase, w^{α}, were calculated with mass balances. The mass fraction of PMMA in the PCL-rich phase (β), $w^{\beta}{}_{PMMA}$, was equal to 0.029. So, the mass fraction of PCL in the β phase ($w^{\beta}{}_{PCL}$) was 0.971. Finally, w^{α} was equal to 0.244. With these values, we have studied the additivity of specific volumes.

3.2. Modelling Results

3.2.1. Theoretical background. The lattice model of SL, which was developed to describe the thermodynamic properties of pure fluids and their solutions, is comprised of a Van der Waals-type attractive term with a lattice-gas repulsive term. As a function of reduced variables, the SL equation of state is expressed as[6,7]

$$\overline{\rho}^2 + \overline{P} + \overline{T}\left[\ln(1-\overline{\rho}) + \left(1 - \frac{1}{r}\right)\overline{\rho}\right] = 0, \tag{1}$$

where r is the number of lattice sites occupied by a molecule, and $\overline{\rho}$, $\overline{P}$, and $\overline{T}$ are the reduced density, pressure, and temperature, respectively. These reduced variables are defined as:

$$\overline{T} = \frac{T}{T^*} \quad \overline{P} = \frac{P}{P^*} \quad \overline{\rho} = \frac{\rho}{\rho^*}, \tag{2}$$

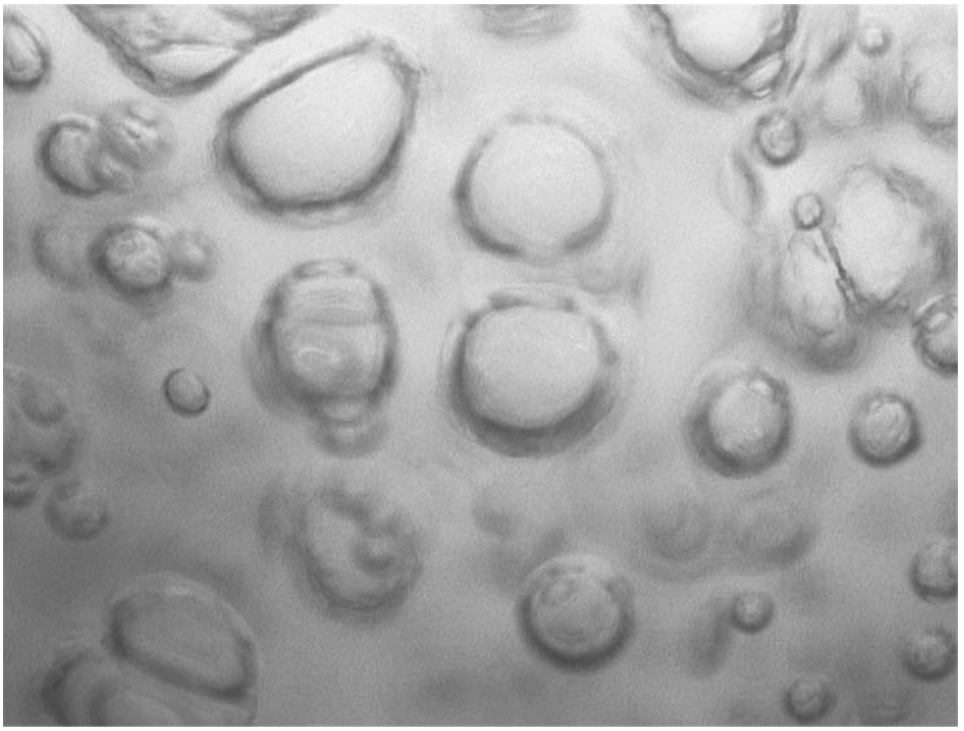

Figure 8. Optical microscope picture of mixture M1 at 180°C.

where ρ, P, and T are the solution density, system pressure, and absolute temperature, respectively; while ρ^*, P^*, and T^* are the corresponding scaling parameters. A pure fluid can be completely characterized by the three scaling parameters (ρ^*, P^*, T^*), or by three molecular parameters, i.e., the interaction energy (ε), the closed-packed molar volume (ν), and the molecular size parameter (r). The relationships among these parameters are

$$T^* = \frac{\varepsilon}{R} \quad P^* = \frac{\varepsilon}{\nu} \quad r = \frac{M P^*}{R T^* \rho^*}, \tag{3}$$

where M and R are the molecular weight and the gas constant, respectively. In the SL theory, the hard-core volume of the polymer segment ($1/\rho^*$), which means the specific volume of the occupied lattice sites, is fixed and can not be chosen arbitrarily, in contrast to other lattice models.[16]

After adjusting the scaling parameters for pure homopolymers (as described below), it is necessary to define scaling parameters for mixtures and copolymers. Calculations were performed using quadratic mixing rules for both parameters, ε and ν, which allows the best correlation of data with a set of binary parameters:[15,47–51]

As a first hypothesis, we assumed the hard-core volumes were additive; so, we supposed that the interaction parameters were the same for both phases

$$\nu_{mix} = \sum\sum \phi_i \, \phi_j \, \nu_{ij} \text{ and } \varepsilon_{mix} = \frac{1}{\nu_{mix}} \sum\sum \phi_i \, \phi_j \, \varepsilon_{ij} \, \nu_{ij} \tag{4}$$

with $\nu_{ij} = \frac{1}{2}(\nu_{ii} + \nu_{jj})(1 - l_{ij})$ and $\varepsilon_{ij} = (\varepsilon_{ii}\varepsilon_{jj})^{1/2}(1 - k_{ij})$,

where ϕ_i is the volume fraction of component i, v_{ii} is the pure i-component characteristic volume, ε_{ii} is the pure i-component interaction energy, and k_{ij} and l_{ij} are lattice-fluids binary parameters of mixtures for energy and volume, respectively.

Orbey et al.[49] compared the ability of different equations of state to simulate phase equilibria in polymer production processes. They concluded that the use of two binary interaction parameters improves the prediction capability of the SL model. For the r value the combination rule is:[52]

$$\frac{1}{r} = \sum \frac{\phi_i}{r_i} \qquad (5)$$

$$\text{with } \phi_i = \frac{w_i / \rho_i^*}{\sum w_j / \rho_j^*}$$

where w_i and ϕ_i are mass and volume fractions of the component i.

3.2.2. Scaling parameters of pure homopolymers. The first step in this study was to analyze the behaviors of the pure homopolymers in order to determine their scaling parameters. For this purpose, the following method of parameter estimation was used. From the experimental PVT data in the liquid state, a table with the values of density (ρ) and temperature (T) for each pressure (P), was built up. Then, a nonlinear least-square fit was carried out by minimizing the following expression:

$$S = \frac{\sum_{i=1}^{N} (\rho_{experimental} - \rho_{calculated})^2}{N_t} \qquad (6)$$

where $\rho_{experimental}$ and $\rho_{calculated}$ are the density measured and predicted by Eq. (1) at given T and P, and N_t is the number of experimental points. The minimum of the S function was searched by using an optimization program that operated over the scaling parameters.

Table 6 lists the scaling parameters obtained for PMMA and PCL, while the goodness of the fit for the specific volumes is shown in Fig. 9. There is some discrepancy in the scaling parameters reported in the literature for PMMA.[7–8,53] The range for T^* is from 696 to 758 K, for P^* from 500 to 671 MPa, and for ρ^* from 1246 to 1300 kg m^{-3}. The scaling parameters reported for PCL are 641 K, 540.1 MPa, and 1182 kg m^{-3}, for T^*, P^*, and ρ^* respectively.[54] Note that the P^* and ρ^* parameters obtained in this study are similar to those previously reported for the same homopolymers, whereas the T^* parameters are lower but of the same order. It is pertinent to mention that Orbey et al. found that different sets of the three input parameters in the SL equation of state gave equally acceptable pure component property estimates.[49]

Table 6
Scaling parameters of homopolymers

Polymer	T^* (K)	P^* (MPa)	ρ^* (kg.cm^{-3})	ε (J.mol^{-1})	v (cm^3.mol^{-1})
PMMA13	573.29	556.47	1,283.32	4,766.33	8.56
PCL14	486.46	540.63	1,206.11	3,894.74	7.20

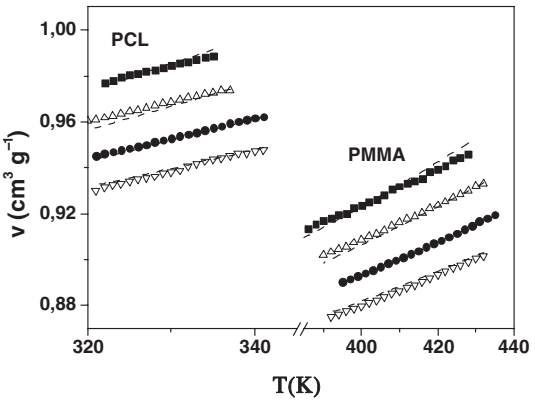

Figure 9. Predictions of Sanchez-Lacombe (SL) equation of state for the specific volumes in the liquid state of the homopolymers. Experimental points: (■) 0.1, (Δ) 20, (●) 40 and (▽) 60 MPa. Predicted values (---).

3.2.3. Lattice-fluid binary parameters. As a hypothesis, we assume that the parameters k_{ij} and l_{ij} do not depend on the composition, and that the molecular weight of the homopolymers in the mixtures and the size of the blocks in the copolymers are sufficiently high that they do not influence these parameters. Nevertheless, PVT data of mixtures and copolymers were correlated separately as it is feasible to suppose that the chemical bonds between the blocks increased the compatibility and diminished the interaction parameter. As pointed out by Nicolas et al.,[53] k_{ij} and l_{ij} show appreciable temperature dependence and they could be well correlated with equations of the form $a + b/T$.[8]

To obtain a and b factors of the lattice-fluid binary parameters, a method of parameter estimation by nonlinear least-square optimization similar to that used to determine the scaling parameters of the pure homopolymers was used. The scaling parameters obtained for the pure homopolymers were used to solve simultaneously Eqs. (1), (4), and (5) and to calculate the density values ($\rho_{calculated}$) of the mixtures or block copolymers. These values were then used in Eq. (6) to determine the factors a and b of each lattice-fluid binary parameter. The results are shown in Table 7 and the corresponding l_{ij} and k_{ij} are plotted in Fig. 10. For both lattice-fluid binary parameters, those for the mixtures were higher than those for the block copolymers, suggesting that the copolymerization process increased the compatibility between the two components. As an example, the goodness of the fit is shown in Fig. 11 for the mixture M2 and for the block copolymer MC2.

Regardless of the composition thereof, all mixtures were represented by one set of parameters whereas all block copolymers were represented by a different set. Thus, we

Table 7
Lattice-fluid binary parameters for mixtures and block copolymers

	k_{ij}		l_{ij}	
	a	b(K)	a	b(K)
Mixtures	−0.456	196.07	2.142	−794.90
Copolymers	−0.637	236.17	2.440	−964.36

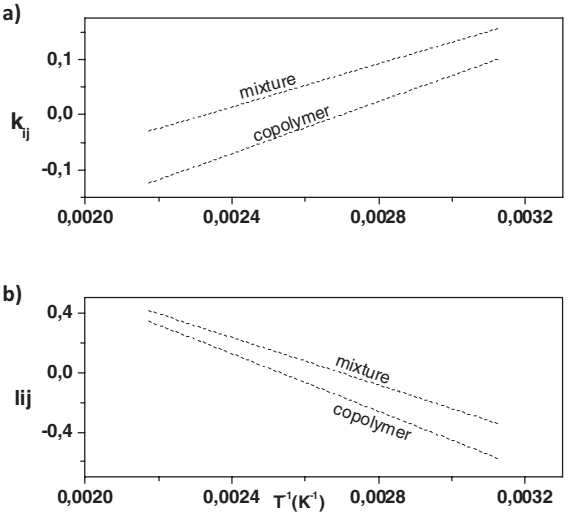

Figure 10. Lattice-fluids binary parameters plotted vs. 1/*T*.

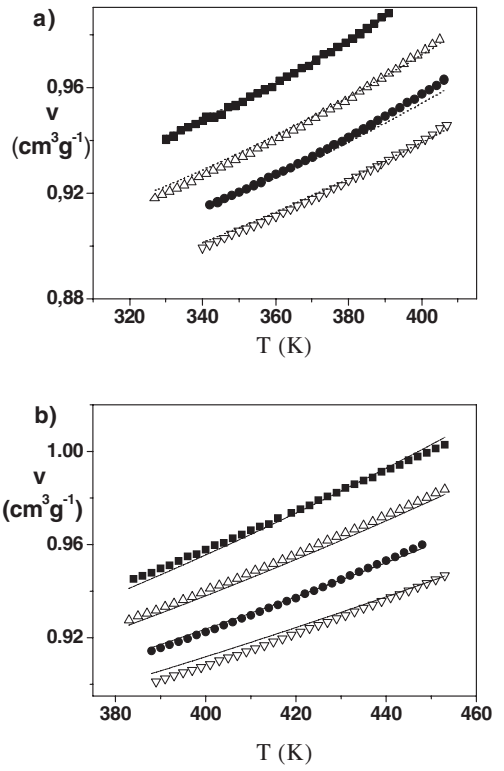

Figure 11. Predictions of SL equation of state for the specific volumes in the liquid state of: (a) M2, and (b) MC2. Experimental points: (■) 0.1, (Δ) 20, (●) 40 and (▽) 60 MPa. Predicted values (---).

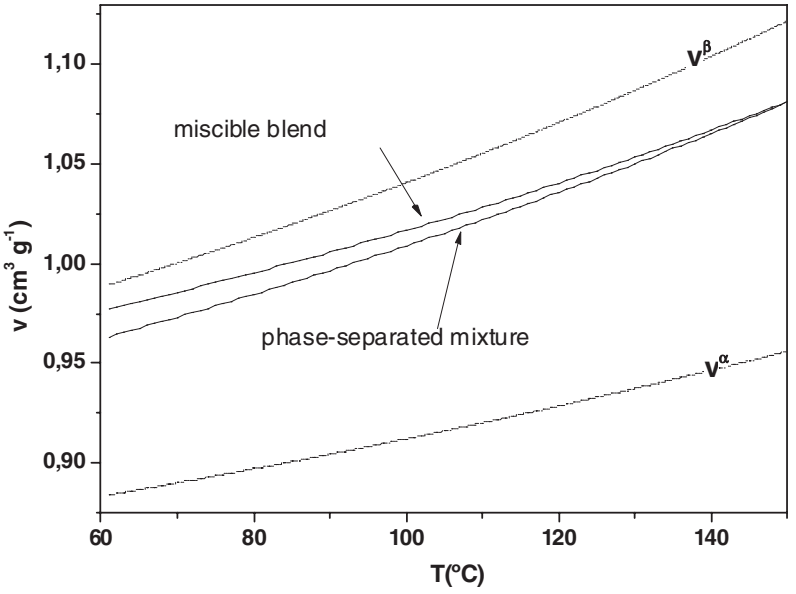

Figure 12. The dotted lines show the predicted specific volumes of each phase, v^α and v^β. The solid lines represent the total predicted volume of the mixture M1 considering it to be miscible blend or a phase-separated mixture.

can conclude that our supposition that the lattice-fluid binary parameters do not depend on composition is valid for the studied systems.

3.2.4. Specific volumes of phase-separated mixture. In the following, we compare the predicted specific volume of the M1 mixture with that arising from the combination of the predicted volumes of each phase. The predicted values of specific volume of each phase are shown in Fig. 12 together with the calculated specific total volumes of a mixture with mass fraction of PMMA equal to 0.25 obtained (a) by considering the mixture as homogeneous

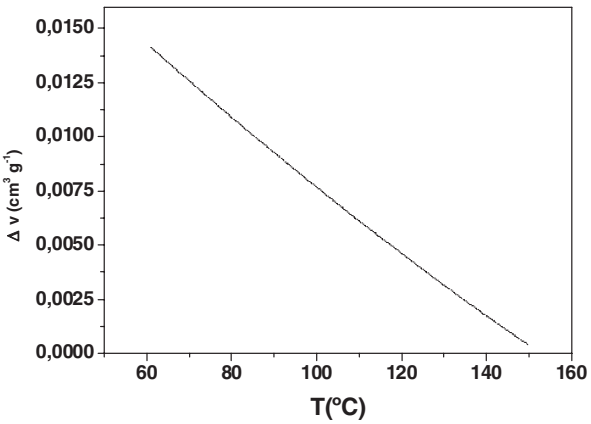

Figure 13. Deviations from the specific volume additivity law.

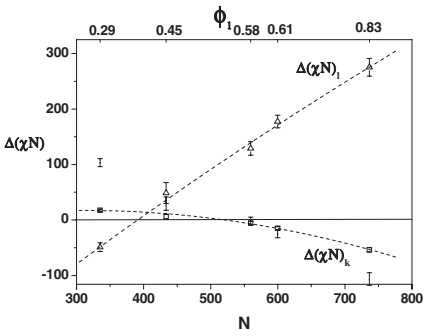

Figure 14. $\Delta(\chi N)$ values from: lattice-fluids binary parameter for energy (□), lattice-fluids binary parameter for volume (Δ).

or (b) by combining the specific volumes of each phase through the following mass balance:

$$\mathrm{v} = \mathrm{v}^{\alpha}\ \mathrm{w}^{\alpha} + \mathrm{v}^{\beta}\ (1 - \mathrm{w}^{\alpha})\,. \tag{7}$$

The difference between the two calculations, Δv, is shown in Fig. 13. Deviations are of the same order of magnitude as those determined by Arce and Aznar for miscible blends of poly(ethylene oxide) and poly(ether sulfone) by using the SL equation.[55] The small differences obtained between the two calculations suggest that our hypothesis of specific volume additivity law is valid.

3.2.5. Comparison with Flory-Huggins interaction parameter. In spite of the controversy in the meaning of the lattice parameters k_{ij} and l_{ij}, we are interested in relating these parameters with the interaction parameter of Flory–Huggins, χ.[16–18] With this objective in mind, we compared the χN values at the $\mathrm{TODT_{app}}$ arising from the phase diagram of block copolymers predicted by Leibler (listed in Table 5) with the $k_{ij}N$ and $l_{ij}N$ values calculated by using the $\mathrm{TODT_{app}}$ temperatures in the expressions of the form $a + b/T$ obtained for k_{ij} and l_{ij} (Table 7). The differences between $\chi N_{LEIBLER}$ and $k_{ij}N$ ($\Delta(\chi N)_k$), and between $\chi N_{LEIBLER}$ and $l_{ij}N$ ($\Delta(\chi N)_l$), are plotted as a function of N in Fig. 14. The results show that the lattice-fluids binary parameter of volume (l_{ij}) was not adequate as an interaction χ-parameter. The smaller difference obtained with the product $k_{ij}N$ allows us to think that the lattice-fluids binary parameter of energy is a better representation of the Flory–Huggins interaction parameter. Although the term $\Delta(\chi N)$ has negative values for copolymers of high N, Fredrickson and Helfand[56] and later Barrat and Fredrickson[57] reformulated Leibler's mean-field theory to include fluctuations which effectively raised the value of $(\chi N)_{\mathrm{TODT}}$.

4. Conclusions

Firstly, we can conclude, in accord with Maurer et al.,[4] that a single set of lattice fluid parameters cannot be used to equally describe the phase behavior of mixtures and block copolymers. As we adjust all data of mixtures with a single set of lattice-binary parameters and all data of block copolymers with another single set, it can be concluded that both l_{ij} and k_{ij} do not depend on the composition for this system. This result, plus the fact that the additivity law of specific volumes can be suitably applied for this system, allowed us to model the behavior of an immiscible blend with the SL equation of state. As expected,

the block copolymer parameters showed a more compatible system due to the chemical linkage between the homopolymers.

By comparing lattice-fluid binary parameters with the Flory–Huggins interaction parameter determined with Leibler's theory we conclude that binary parameter of energy is a better representation of the Flory–Huggins interaction parameter.

Nevertheless future work with mixtures of partially miscible homopolymers and the corresponding block copolymers is necessary to be able to compare SL's results with those which ensue from the application of Flory–Huggins's equation.

Acknowledgments

The authors thank Prof. Phillip H. Geil for his valuable suggestions.

References

1. Flory, P.J. Thermodynamics of high polymer solutions. J. Chem. Phys. **1942**, *10*, 51.
2. Huggins, M.L. Some properties of solutions of long-chain compounds. J. Phys. Chem. **1942**, *46*, 151.
3. Lohse, D.J.; Fetters, L.J.; Doyle, M.J.; Wang, H.-C.; Kow, C. Miscibility in blends of model polyolefins and corresponding diblock copolymers: Thermal analysis studies. Macromolecules **1993**, *26*, 3444.
4. Maurer, W.W.; Bates, F.S.; Lodge, T.P.; Almdal, K.; Mortensen, K.; Fredrickson, H. Can a single function for χ account for block copolymer and homopolymer blend phase behavior? J. Chem. Phys. **1998**, *108*, 2989.
5. Leibler, L. Theory of microphase separation in block copolymers. Macromolecules **1980**, *13*, 1602.
6. Sanchez, I.C.; Lacombe, R.H. An elementary molecular theory of classical fluids. Pure fluids. J. Phys. Chem. **1976**, *80*, 2352.
7. Sanchez, I.C.; Lacombe, R.H. Statistical thermodynamics of polymer solutions. Macromolecules **1978**, *11*, 1145.
8. Wen, G.; Sun, Z.; Shi, T.; Yang, J.; Jiang, W.; An, L.; Li, B. Thermodynamics of PMMA/SAN blends: application of the Sanchez-Lacombe lattice-fluid theory. Macromolecules **2001**, *34*, 6291.
9. Callaghant, T.A.; Paul, D.R. Interaction energies for blends of poly(methy1 methacrylate), polystyrene, and poly(α-methylstyrene) by the critical molecular weight method. Macromolecules **1993**, *26*, 2439.
10. Yoo, J.E.; Kim, Y.; Kim, C.K.; Lee, J.W. Phase behavior of binary and ternary blends having the same chemical components and compositions. Macromol. Res. **2003**, *11*, 303.
11. Chen, X.; Sun, Z.; Yin, J.; An, L. Thermodynamics of blends of PEO with PVAc: application of the Sanchez–Lacombe lattice-fluid theory. Polymer **2000**, *41*, 5669.
12. Jeon, K.S.; Char, K.; Walsh, D.J.; Kim, E. Thermodynamics of mixing estimated by equation-of-state parameters in miscible blends of polystyrene and tetramethyl bisphenol-A polycarbonate. Polymer **2000**, *41*, 2839.
13. Paul, D.R. Polymer-polymer interactions. Pure Appl. Chem. **1995**, *67*, 977.
14. Chu, J.H.; Paul, D.R. Blends of SAN with methyl methacrylate copolymers of 2-hydroxyethyl methacrylate and 4-methacryloxyethyl trimellitic anhydride. Polymer **2000**, *41*, 7193.
15. Sato, Y.; Hashiguchi, H.; Inohara, K.; Takishima, S.; Masuoka, H. PVT properties of polyethylene copolymer melts. Fluid Phase Equil. **2007**, *257*, 124.
16. Rudolf, B.; Cantow, H.J. Description of phase behavior of polymer blends by different equation-of-state theories. 1. Phase diagrams and thermodynamic reasons for mixing and demixing. Macromolecules **1995**, *28*, 6586.
17. Tao, Y.; Wells, P.S.; Yi, X.; Yun, K.S.; Parcher, J.F. Lattice-fluid model for gas-liquid chromatography. J. Chromatogr. A **1999**, *862*, 49.

18. Martin, T.M.; Young, D.M. Correlation of the glass transition temperature of plasticized PVC using a lattice fluid model. Polymer **2003**, *44*, 4747.
19. Yang, J.; An, L.; Dong, L.; Teng, F.; Feng, Z. Theoretical estimation of thermodynamic properties of the system PS/PPO on the basis of modified combining rule of Sanchez–Lacombe lattice fluid model. Eur. Polym. J. **2002**, *38*, 2083.
20. Higgins, J.S.; Tambasco, M.; Lipson, J.E.G. Polymer blends; stretching what we can learn through the combination of experiment and theory. Prog. Polym. Sci. **2005**, *30*, 832.
21. Tambasco, M.; Lipson, J.E.G.; Higgins, J.S. New routes to the characterization and prediction of polymer blend properties. Macromolecules **2004**, *37*, 9219.
22. Jeon, M.Y.; Kim, C.K. Phase behavior of polymer/diluent/diluent mixtures and their application to control microporous membrane structure. J. Membr. Sci. **2007**, *300*, 172.
23. Sato, T.; Tsujita, Y.; Takizawa, A.; Kinoshita, T. Miscibility and volume changes of mixing in the poly(vinyl chloride)/poly(methyl methacrylate) blend system. Macromolecules **1991**, *24*, 158.
24. Ougizawa, T.; Dee, G.T.; Walsh, D.J. Pressure-volume-temperature properties and equation of state in polymer blends: characteristic parameters in polystyrene/poly(vinyl methyl ether) mixtures. Macromolecules **1991**, *24*, 3834.
25. Elvira, C.; Fanovich, A.; Fernández, M.; Fraile, J.; San Román, J.; Domingo, C. Evaluation of drug delivery characteristics of microspheres of PMMA-PCL-cholesterol obtained by supercritical-CO_2 impregnation and by dissolution-evaporation techniques. J. Contr. Rel. **2004**, *99*, 231.
26. Levent Demirel, A.; Değirmenci, M.; Yusuf Yağcı, Y. Atomic force microscopy investigation of asymmetric diblock copolymer morphologies in thin films. Eur. Polym. J. **2004**, *40*, 1371.
27. Iannace, S.; De Luca, N.; Nicolais, L.; Carfagna, C.; Huang, S.J. Physical characterization of incompatible blends of poly(methyl methacrylate) and polycaprolactone. J. Appl. Polym. Sci. **1990**, *41*, 2691.
28. Levy, M. Living Polymers – 50 years of evolution. Bull. Israel Chem. Soc. **2005**, *18*, 20.
29. Xu, Y.; Pan, C.; Tao, L. Block and star block copolymers by mechanism transformation. II. Synthesis of poly (DOP-*b*-St) by combination of ATRP and CROP. J. Polym. Sci., Part A: Polym. Chem. **2000**, *38*, 436.
30. Hedrick, J.L.; Trollsås, M.; Hawker, C.J.; Atthoff, B.; Claesson, H.; Heise, A.; Miller, R.D.; Mecerreyes, D.; Jérôme, T.; Dubois, P. Ring opening and atom transfer radical polymerization. Macromolecules **1998**, *31*, 8691.
31. Desjardins, S.Y.; Cavell, K.J.; Jin, H.; Skelton, B.W.; White, A.H. Insertion into the nickel-carbon bond of N—O chelated arylnickel(II) complexes. The development of single component catalysts for the oligomerisation of ethylene. J. Organomet. Chem. **1996**, *515*, 233.
32. Wang, D.; Peng, Z.; Liu, X.; Tong, Z.; Wang, C.; Ren, B. Synthesis and micelle formation of triblock copolymers of poly(methyl methacrylate)-*b*-poly(ethylene oxide)-*b*-poly(methyl methacrylate) in aqueous solution. Eur. Polym. J. **2007**, *43*, 2799.
33. Jiang, H.; He, J.; Tao, Y.; Yang, Y. Synthesis and characterization of star-branched poly(ε-caprolactone). Polymer J. **2003**, *35*, 598.
34. Wang, G.; Shi, Y.; Fu, Z.; Yang, W.; Huang, O.; Zhang, Y. Controlled synthesis of poly(ε-caprolactone)-*graft*-polystyrene by atom transfer radical polymerization with poly(ε-caprolactone-*co*-α-bromo-ε-caprolactone) copolymer as macroinitiator. Polymer **2005**, *46*, 10601.
35. Xiaong, H.; Zheng, J.X.; Van Horn, R.M.; Jeong, K.U.; Quirk, R.P.; Lotz, B.; Thomas, E.L.; Brittain, W.J.; Chen, S.Z.D. A new approach in the study of tethered diblock copolymer surface morphology and its tethering density dependence. Polymer **2007**, *48*, 3732.
36. Iroh, J.O. Poly(ε-caprolactone). In *Polymer Data Handbook*; Mark, J.E., Ed.; Oxford University Press Inc.: New York, **1999**, pp 361–362.
37. Helfand, E. Block copolymer theory. III. Statistical mechanics of the microdomain structure. Macromolecules **1975**, *8*, 552.
38. Seeger, A.; Freitag, D.; Freidel, F.; Luft, G. Melting point of polymers under high pressure: Part I: influence of the polymer properties. Thermochim. Acta. **2004**, *424*, 175.

39. Kilburn, D.; Dlubek, G.; Pionteck, J.; Ford, D.B.; Alam, M.A. Microstructure of free volume in SMA copolymers I. Free volume from Simha-Somcynsky analysis of PVT experiments. Polymer **2005**, *46*, 859.
40. Wang, F.; Saeki, S.; Yamaguchi, T. Temperature and pressure dependence of thermal expansion coefficient and thermal pressure coefficient for amorphous polymers. Polymer **1997**, *38*, 3485.
41. Kilburn, D.; Dlubek, G.; Pionteck, J.; Alam, M.A. Free volume in poly(*n*-alkyl methacrylate)s from positron lifetime and PVT experiments and its relation to the structural relaxation. Polymer **2006**, *47*, 7774.
42. Hsu, S.L. Poly(methyl methacrylate). In *Polymer Data Handbook*; Mark, J.E., Ed.; Oxford University Press Inc.: New York, **1999**, pp 656–657.
43. Fox, T.G. Influence of diluent and of copolymer composition on the glass temperature of a polymer system. Bull. Am. Phys. Soc. **1956**, *2*, 123.
44. Grimau, M.; Laredo, E.; Pérez, M.C.; Bello, A. Study of dielectric relaxation modes in poly(ε-caprolactone): Molecular weight, water sorption, and merging effects. J. Chem. Phys. **2001**, *114*, 6417.
45. Hashimoto, T.; Ogawat, T.; Sakamoto, N.; Ichimiya, M.; Kim, J.K.; Han, C.D. Small-angle X-ray scattering and rheological studies on the ordering process of cylindrical microdomains in a polystyrene-*block*-polyisoprene copolymer. Polymer **1998**, *39*, 1573.
46. Floudas, G.; Pakula, T.; Velis, G.; Sioula, S.; Hadjichristidis, N. Equilibrium order-to-disorder transition temperature in block copolymers. J. Chem. Phys. **1998**, *108*, 6498.
47. Hamley, I.W.; Castelletto, V.; Yang, Z.; Price, C.; Booth, C. Melt phase behavior of poly(oxyethylene)-poly(oxypropylene) diblock copolymers. Macromolecules **2001**, *34*, 4079.
48. Xu, J.T.; Patrick, J.; Fairclough, A.; Mai, S.M.; Chaibundit, C.; Mingvanish, M.; Booth, C.; Ryan, A.J. Crystallization behavior of oxyethylene/oxybutylene diblock and triblock copolymers. Polymer **2003**, *44*, 6843.
49. Orbey, H.; Bokis, C.P.; Chen, C.C. Equation of state modeling of phase equilibrium in the low-density polyethylene process: the Sanchez–Lacombe, Statistical Associating Fluid yheory, and Polymer-Soave-Redlich-Kwong equations of state. Ind. Eng. Chem. Res. **1998**, *37*, 4481.
50. McHugh, M.A.; Krukonis, V.J. *Supercritical Fluid Extraction: Principles, Practice,* 2nd ed.; Butterworth Heinemann: Boston, 1994.
51. Neau, E. A consistent method for phase equilibrium calculation using the Sanchez-Lacombe lattice-fluid equation-of-state. Fluid Phase Equil. **2002**, *203*, 133.
52. Colussi, S.; Elvassore, N.; Kikic, I. A comparison between semi-empirical and molecular-based equations of state for describing the thermodynamic of supercritical micronization processes. J. Supercrit. Fluid. **2006**, *39*, 118.
53. Nicolas, C.; Neau, E.; Meradji, S.; Raspo, I. The Sanchez-Lacombe lattice-fluid model for the modeling of solids in supercritical fluids. Fluid Phase Equil. **2005**, *232*, 219.
54. Múgica, A.; Remiro, P.M.; Cortázar, M. Lattice fluid theory in the analysis of interaction parameters and phase behaviour of blends involving copolymers of cyclohexyl methacrylate, methyl methacrylate and various styrene derivatives. Polymer **2000**, *41*, 5257.
55. Arce, P.F.; Aznar, M. Modeling of thermodynamic behavior of PVT properties and cloud point temperatures of polymer blends and polymer blend + carbon dioxide systems using noncubic equations of state. Fluid Phase Equil. **2009**, *286*, 17.
56. Fredrickson, G.H.; Helfand, E. Fluctuation effects in the theory of microphase separation in block copolymers. J. Chem. Phys. **1987**, *87*, 697.
57. Barrat, J.; Fredrickson, G.H. Collective and single chain correlations near the block copolymer order-disorder transition. J. Chem. Phys. **1991**, *95*, 1281.